NASA TECHNICAL MEMORANDUM

NASA TM X-1488

NASA TM X-1488

FLIGHT EVALUATION OF AN ELECTROSTATIC ACCELEROMETER FOR MEASUREMENT OF LOW-LEVEL ORBITAL ACCELERATIONS

by Daniel J. Lesco

Lewis Research Center

Cleveland, Ohio

NATIONAL AERONAUTICS AND SPACE ADMINISTRATION • WASHINGTON, D. C. • JANUARY 1968

NASA TM X-1488

FLIGHT EVALUATION OF AN ELECTROSTATIC ACCELEROMETER FOR MEASUREMENT OF LOW-LEVEL ORBITAL ACCELERATIONS

By Daniel J. Lesco

Lewis Research Center
Cleveland, Ohio

NATIONAL AERONAUTICS AND SPACE ADMINISTRATION

For sale by the Clearinghouse for Federal Scientific and Technical Information
Springfield, Virginia 22151 – CFSTI price $3.00

FLIGHT EVALUATION OF AN ELECTROSTATIC ACCELEROMETER FOR MEASUREMENT OF LOW-LEVEL ORBITAL ACCELERATIONS

by Daniel J. Lesco

Lewis Research Center

SUMMARY

The results of the first flight test of an experimental electrostatic accelerometer are presented. Measurements of liquid-hydrogen venting accelerations as low as 6×10^{-5} g were obtained aboard an orbiting Saturn S-IVB stage. Comparison of the accelerometer readings is made with other flight measurements. The time correlation between output data and attitude control system firings is also described.

INTRODUCTION

For the accurate measurement of low-level orbital accelerations of 10^{-4} g and lower, an extremely sensitive accelerometer with a low null bias (output at conditions of zero input) is required. A conventional accelerometer cannot be used because the null bias would be of the same order of magnitude as the accelerations to be measured. This bias results from the coupling into the accelerometer sensitive axis of the mechanical cross-axis forces required to support the acceleration sensing element (the accelerometer proof mass).

An accelerometer designed to eliminate the null bias problem is the miniature electrostatic accelerometer (MESA) (ref. 1). The advantage of an electrostatically suspended accelerometer is the capability to reduce the cross-axis suspension forces for operation in a low-acceleration environment simply by reducing suspension voltages. The major disadvantage is the inability to calibrate the accelerometer in the environment in which it will operate. Ground testing requires the increase of cross-axis suspension forces to support the proof mass in a 1-g environment. The ground calibrations for the accelerometer are assumed, on the basis of accelerometer design, to hold for orbital operation. The null bias is theoretically reduced in proportion to the reduction in cross-axis suspension forces.

The use of an electrostatic accelerometer was employed in the measurement of liquid-hydrogen venting accelerations aboard an orbiting Saturn S-IVB (AS-203). The AS-203 was the first flight test of the Lewis Research Center contract-developed accelerometer.

On Saturn S-IVB (AS-203), orbited in July 1966, experiments were performed to determine the effects of near-zero acceleration forces on the liquid hydrogen in the booster fuel tanks. Venting jets were used to accelerate the vehicle in an attempt to seat the liquid hydrogen near the fuel pumps. The measurements and observations of the liquid-hydrogen behavior were compared with the low-level accelerations produced by the vent thrusting (on the order of 10^{-5} g). The MESA was requested by the NASA Marshall Space Flight Center to fulfill the instrumentation needs and to provide a flight evaluation of an electrostatic accelerometer. This report describes the results of the AS-203 flight test of the MESA.

MINIATURE ELECTROSTATIC ACCELEROMETER

The electrostatic accelerometer is an instrument designed for measurement of accelerations of less than 10^{-3} g in a low-gravity environment. In conventional accelerometers, mechanical cross-axis support for the proof mass is provided for operation in a 1-g gravitational field and, in space applications, for withstanding the high-gravity vibration and shock levels experienced during launch. Because of the finite tolerances of fabrication, a small percentage of the cross-axis support forces (on the order of 10^{-5} g minimum, ref. 1) are coupled into the accelerometer sensitive axis as a null bias. If the cross-axis forces in an accelerometer could be reduced when the accelerometer is operated in a low-g environment (as in Earth orbit), the null bias of the accelerometer would be proportionately decreased. The electrostatic accelerometer, the proof mass of which is supported electrostatically, provides a solution to the null bias problem.

Principles of Operation

A complete description of the operation of the miniature electrostatic accelerometer (MESA) used is given in reference 1. In figure 1, the major mechanical components of the accelerometer structure are shown. All the parts are fabricated to the tolerances necessary for an accurate instrument based on electrostatic principles.

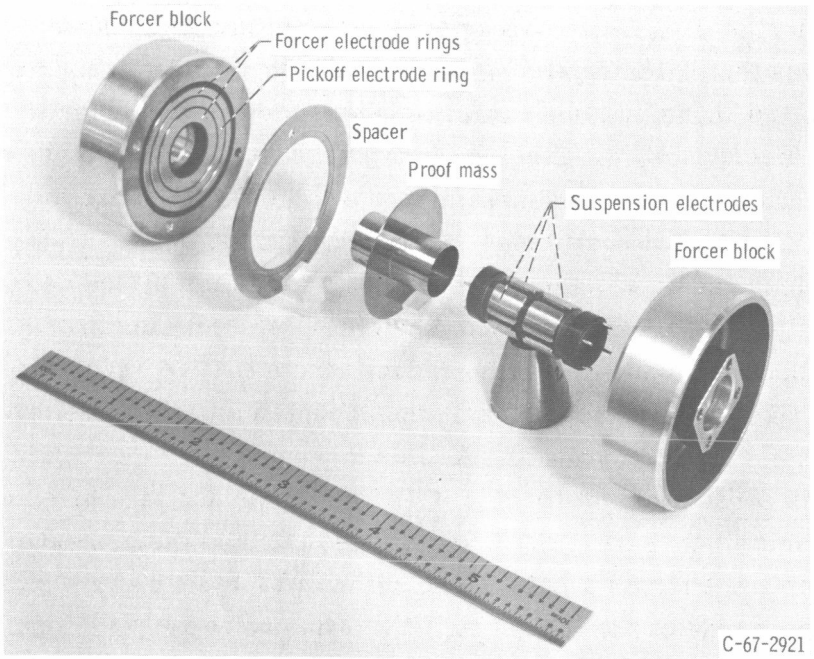

Figure 1. - Major mechanical elements of miniature electrostatic accelerometer (MESA).

Cross-axis suspension forces. - The basic principle for suspending the proof mass of the accelerometer is the attractive force between the plates of a charged capacitor. This electrostatic force is related to the voltage V across the plates and the distance d between the plates by the equation

$$F = K \frac{V^2}{d^2}$$

where K is a constant. Since the force is proportional to V^2, it is always attractive regardless of the polarity of V.

When suspended, the hollow cylindrical proof mass (fig. 1) forms a set of capacitors with corresponding electrode pads on an axial rod within the cylinder. Because the electrostatic forces are inversely proportional to the square of the plate separation, suspension cannot be achieved with a dc voltage across the capacitors. For this case, any external disturbance from suspension equilibrium will result in an increase in the force between the proof mass and the nearer electrode pad together with a decrease in the force from the opposite electrode pad. This positive feedback effect will further disturb the force balance, and suspension will be lost. However, suspension can be achieved with an ac voltage applied across the set of capacitors, each in series with an inductance. If the ac frequency is slightly above the resonant

frequency of the series capacitance-inductance, the voltage (and, hence, the electrostatic force) across the plates can be made to decrease as the gap decreases. If the gap between the proof mass and one capacitor electrode pad, together with the associated force, decreases, the increasing gap between the proof mass and the pad on the opposite side of the axial rod causes an increase in electrostatic forces, which returns the proof mass to an equilibrium condition of suspension.

The magnitude of the ac voltage supplied to the capacitor plates determines the maximum external cross-axis forces which can be tolerated. In a low-g environment, therefore, the suspension voltage may be reduced from that required for suspension in a 1-g field. The reduction in suspension forces coupled into the accelerometer sensitive axis results in a decrease in null bias.

Sensitive-axis constrainment forces. - The detection and measurement of the proof mass movement in the sensitive-axis direction also utilizes electrostatic forces. A flange on the proof mass forms a pair of capacitors with a concentric pickoff electrode ring situated on each side of the flange (fig. 1). The two capacitors form two legs of a capacitive bridge circuit which measures the position of the flange relative to a null position. If external accelerations so move the proof mass that the bridge output exceeds a set trigger level, voltage pulses are applied to one set of the concentric forcer rings (in the same planes as the pickoff rings) to force the proof mass toward the null position. To maintain the proof mass at ground potential, positive and negative pulses of equal amplitude and width are applied simultaneously to two forcer rings on the same forcer block. The frequency of force pulses required to keep the proof mass near null is proportional to the external acceleration. The full-scale capability of the accelerometer is a function of the magnitude of the force pulse voltage and may be readily varied.

The pulse generation circuitry is voltage and thermally controlled to provide accurate, stable force pulses. These pulses are generated by a saturable magnetic pulse transformer, for which the saturation levels are precisely controlled. The voltage pulses on the secondary of the transformer are produced by alternately switching positive and negative direct current through the transformer primary, which switches the core between its two saturation levels. The output pulse area (in volt-seconds) is stable if the core saturation levels are constant. The pulse voltage amplitude is maintained by precise voltage regulation.

The core saturation levels are maintained constant by controlling the internal core temperature. In uncontrolled operation, an increase in pulse frequency would result in an increase in core heat dissipation and, hence, in core temperature. In the MESA, the tape-wound transformer core is used as both a resistive temperature sensing and a heating element for its own environment. An increase in core temperature decreases the controlled heater current flowing through the core, which thereby lessens the core heater power and maintains a constant temperature.

Since the linearity of the accelerometer output pulse frequency with input acceleration is a function only of the stability of the forces per pulse applied to the proof mass and the stability of the null bias, the measurement error of the instrument is a percentage of reading plus the null bias. The accelerometer output calibration can, therefore, be expressed by the output scale factor (pulse frequency/full-scale input acceleration) and the null bias scaled for the cross-axis suspension force applied.

Accelerometer electronics for over-range control. - A simplified block diagram of the accelerometer electronics is shown in figure 2. When the output of the capacitance

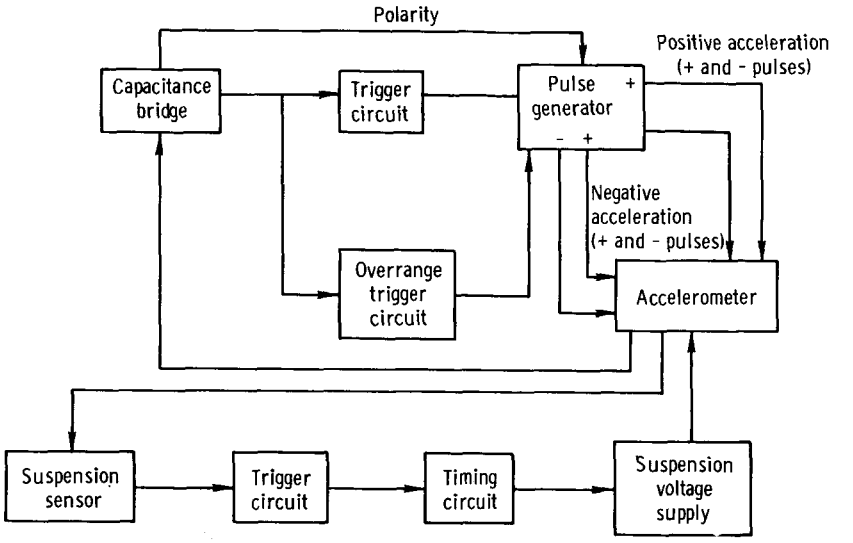

Figure 2. - Accelerometer electronics block diagram.

bridge exceeds the trigger level, force pulses are applied to one set of accelerometer forcer rings so as to oppose the external acceleration, the polarity of which is determined by the bridge. If the bridge output should exceed a second (higher) trigger level, an overrange circuit increases the pulse voltage by a factor of 100 until the bridge output decreases below the overrange trigger level. The purpose of the overrange control is to decrease the recovery time of the accelerometer for large, transient input accelerations.

Similarly, if the proof mass should lose suspension, the suspension sensor initiates a signal, which increases the suspension voltage to overcome transient cross-axis accelerations. The timing circuit recycles the suspension voltage back to the low-level condition until the float remains suspended with the low-level voltages.

Accelerometer Configuration for Saturn AS-203 Flight

For the Saturn AS-203 flight, the cross-axis suspension capability was set for

10^{-3} g. The full-scale sensitive-axis acceleration was also 10^{-3} g to allow reasonably accurate ground calibrations. An average accelerometer output frequency of 4375 counts per second was equivalent to the full-scale reading. The theoretical null bias was 4×10^{-7} g.

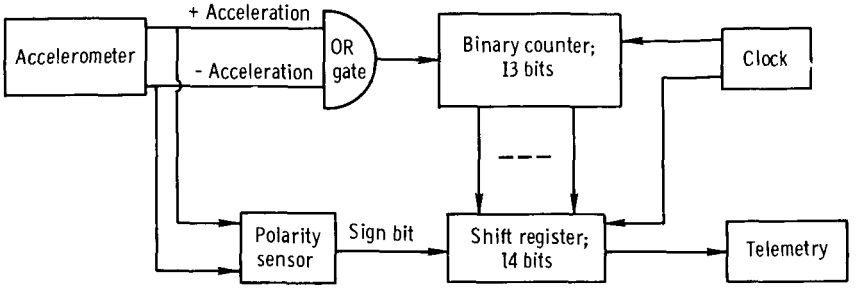

Figure 3. - Data conditioner for accelerometer in AS-203 flight.

Figure 3 shows a block diagram of the accelerometer output data conditioner used on the AS-203 flight. The binary counter accumulated the accelerometer pulse output (for either plus or minus input accelerations) each 1-second period. The count was then transferred to the shift register, along with a polarity bit. The 14-bit binary word was serially shifted to the spacecraft telemetry once each second. Thus, continuous readings of acceleration with a 1-second averaging time were transmitted to the orbital-path ground stations.

The maximum theoretical error in the accelerometer digital output was ±1 percent of the reading $\pm4\times10^{-7}$ g (the null bias), and the output calibration error was an additional ±1 percent of the reading.

The other accelerometer parameters telemetered during the AS-203 flight were

(1) Accelerometer temperature

(2) Proof mass position (amplified output of capacitance bridge)

(3) Analog acceleration output (low-pass filtered pulse output)

ACCELEROMETER FLIGHT DATA FOR SATURN AS-203 FLIGHT

Flight Measurements

Figure 4 is a plot of the digital output of the MESA, averaged over periods of 10 seconds each, as a function of time from the Saturn AS-203 lift-off. The 1-second average data from the accelerometer showed a scatter of over ±50 percent of the 10-second average acceleration data. These fluctuations are thought to be a function

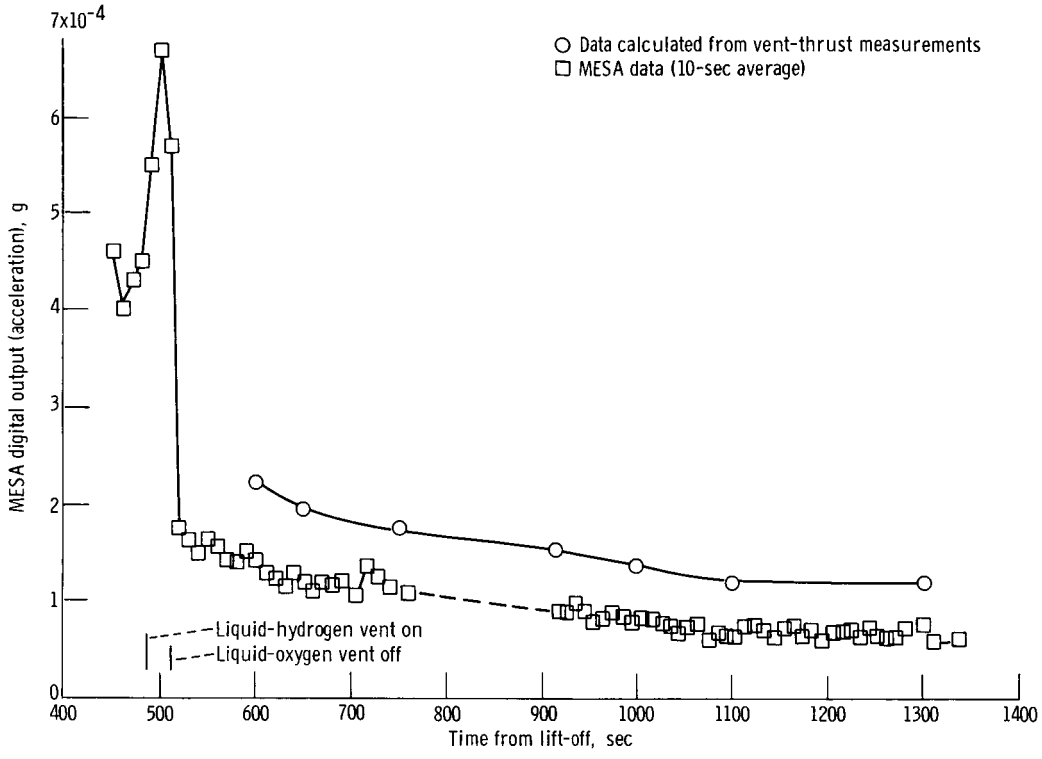

Figure 4. - Saturn S-IVB vehicle orbital acceleration in AS-203 flight.

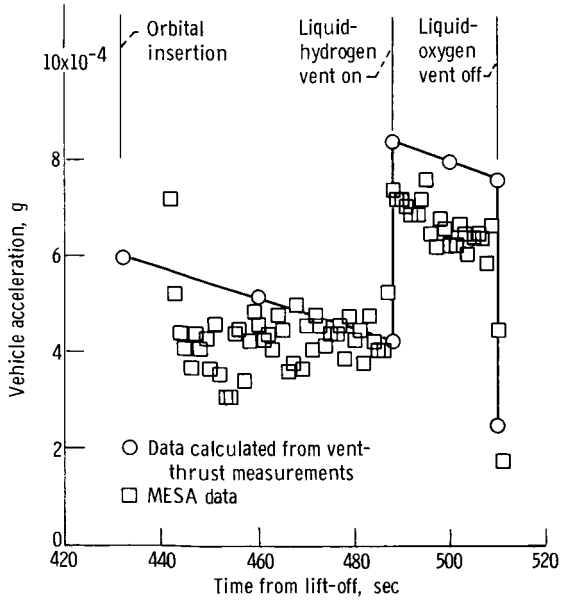

Figure 5. - Vehicle acceleration in AS-203 flight during turn on of liquid-hydrogen venting and turn off of liquid-oxygen venting.

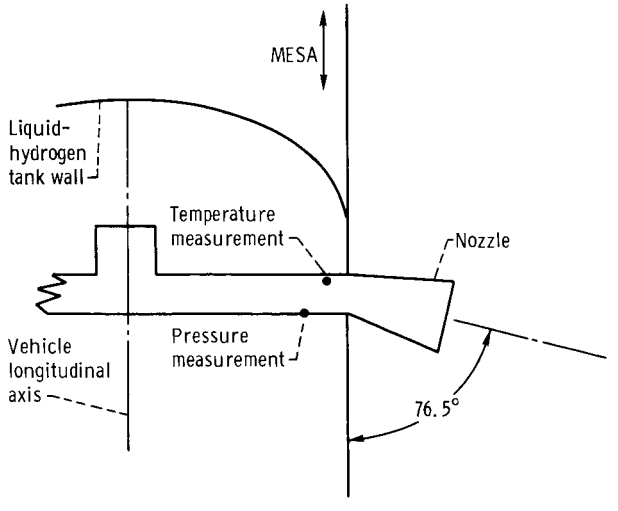

Figure 6. - Schematic diagram of AS-203 liquid-hydrogen continuous vent system and instrumentation.

of attitude control system firings, propellant slosh, and venting system oscillations. After the initial period of transient accelerations, the measured acceleration appears to approach a steady-state level of about 6×10^{-5} g. Two major flight events can be time-correlated with the accelerometer data:

(1) The start of liquid-hydrogen venting at 488 seconds

(2) The shutdown of liquid-oxygen venting at 511 seconds

Figure 5 shows the 1-second average data obtained during these events. The 1-second average MESA data resolves these events to within ±1 second.

Also shown in figures 4 and 5 are AS-203 acceleration data (ref. 2) calculated from vent-thrust magnitudes based on temperature and pressure measurements on the liquid-hydrogen venting system and corrected for vehicle drag accelerations. The accuracy for the thrust-determined data was believed to be ±10 percent; however, a partial failure of the measurement instrumentation did occur. One of the vent pressure transducers exhibited slow response to transient pressure conditions because of suspected blockage of the pressure measurement line.

Figure 6 is a schematic diagram of one of the two vent nozzles of the liquid-hydrogen venting system. Pressure and temperature measurement instrumentation was provided for each nozzle. The vehicle longitudinal acceleration produced by the vent system is a function of the vent thrust angle for a nozzle angle of 76.5°. The figure also shows the relative location of the electrostatic accelerometer.

The MESA was expected to provide acceleration data with an error less than ±2 percent of the reading (due to system and calibration errors). The telemetered system parameters, accelerometer temperature and float position, showed no deviation from the correct operational values. Calculated values for gravity gradient and orbital rate accelerations acting on the MESA were several orders of magnitude less than the measured acceleration and, therefore, can be considered negligible.

The accelerometer data for the initial seconds of the flight after orbital insertion (fig. 5) agree with the vent-thrust calculated acceleration to within 20 percent.

For the time period after liquid-oxygen vent cutoff, the accelerometer data are about 40 percent less than the calculated vent-thrust data. This difference cannot be totally explained with the available AS-203 flight data.

A small fraction of the difference can be accounted for on the basis of attitude control system accelerations. All modes of the control system firings result in short duration, negative (-5×10^{-4} g) accelerations as measured by the MESA. The plot of 10-second average data shown in figure 4 (p. 7) during the time period of 900 to 1300 seconds illustrates a variation of measured acceleration of about 1×10^{-5} g about the average level. If data obtained only while no attitude control system firing occurred were plotted, the acceleration curve would coincide with the positive peak readings of the small amplitude variations. The measured acceleration due to liquid-hydrogen vents

thrusting alone would be 5×10^{-6} g greater than an average acceleration obtained from the plot in figure 4. This correction would reduce the discrepancy in data to about 30 percent.

MESA Error Sources Pertinent to AS-203 Data

The MESA design was studied to determine possible sources for large errors which would not involve complete failure of the accelerometer and would not affect the other telemetered accelerometer outputs. An error in accelerometer measurements could occur from changes in three parameters:

(1) Digital output scale factor (pulses/(sec)(mg))

(2) Null bias

(3) Scale factor linearity

An error in scale factor would result from any changes in the effective electrostatic forces applied to the proof mass to return it to the null position. These changes could originate from either electronic failure or from mechanical damage to the flange on accelerometer proof mass. The only changes that need be considered, in light of the sign of the observed data discrepancy, are those that would have produced larger forces per pulse on the proof mass than were expected. The possible electronic failures include shorting in the primary windings of the transformer which supplies the constant force pulses (either positive or negative polarity pulses). A possible mechanical failure is a bending of the proof mass flange that results in a decrease in the distance between the flange and the forcer rings being pulsed. Both examples would result in a larger amplitude force pulse applied to the proof mass and, hence, a decrease in the output scale factor.

An increase in the null bias from the expected value could result from mechanical damage to the proof mass. The cylindrical section of the proof mass could couple a larger component of the suspension voltage into the sensitive axis if it became damaged during the Saturn lift-off.

On the basis of environmental preflight testing of the MESA, it seems improbable that any of the aforementioned accelerometer failure modes would occur and result in a 30 percent error in acceleration measurement. Calibration tests conducted on the MESA after environmental testing showed changes in the scale factor of only about 1 percent (the calibration accuracy) from the initial calibrations. It is unlikely that a significant calibration change could occur without catastrophic failure or without a significant effect on the proof mass position output.

A change in the scale factor linearity could result from failure in the pulse generator

core temperature control. However, this type failure could not account for large output errors.

Consideration of errors in the digital data conditioner was eliminated since the accelerometer saturation output reading during Saturn lift-off was the correct maximum frequency output of the accelerometer.

The acceleration values calculated from thrust measurements approached 6×10^{-5} g at about 5000 seconds after lift-off, before the first simulated restart of the S-IVB stage, which was the acceleration level approached by the MESA measurements at 1300 seconds.

Attitude-Thrustor - Accelerometer-Data Time Correlation

Further confirmation of proper operation of the accelerometer was supplied through time correlation of the AS-203 flight data with the attitude thrustor (attitude positioning system, APS) firings during the first orbit.

The theoretical acceleration experienced by the accelerometer during APS firings was about -5×10^{-4} g. The firings, however, were of short duration (<1 sec) and, therefore, insufficient to drive the accelerometer float past the negative trigger level.

Data of accelerometer proof mass position (in the sensitive axis) for the first orbital segment over the Canary Island tracking station shows 28 major fluctuations which could be attributed to sudden, relatively large variations in measured acceleration. Of these 28 fluctuations, 25 could be time-correlated to within 1 second (the time resolution of the data readout) of an APS firing. During this period of about 400 seconds, there were a total of 37 APS firings.

Similarly, out of 16 major fluctuations in the 1-second average digital acceleration data, 14 fluctuations could be time-correlated to an APS firing. In all cases, the fluctuations were negative with respect to the average measured acceleration. The decrease in measured acceleration is to be expected from consideration of the angular torques applied to the Saturn vehicle during the APS firings.

These data, though not quantitative, do verify the dynamic sensitivity of the accelerometer and, indirectly, the continuous suspension of the accelerometer float.

System Failure and Probable Causes

Accelerometer data were obtained for the first 1350 seconds of the AS-203 flight (through the Canary Island tracking station coverage). When telemetry coverage over the subsequent tracking station was achieved, all telemetry channels from the accelerometer provided zero readings, except for the accelerometer temperature monitor.

This system failure was attributed to failure of power to or in the accelerometer for the following reasons:

(1) The temperature monitor and accelerometer heaters were supplied from a different power lead than were the remaining accelerometer electronics.

(2) Loss of data from all other channels has a low probability of occurring except for a power failure to the entire system.

(3) A zero output reading for the float position is undefined except for a power failure.

(4) A temporary power interruption of undetermined cause occurred during the preflight accelerometer system checkout. After a short delay, power was restored without any obvious corrective measures. Subsequent checking failed to locate the trouble area.

CONCLUSIONS

A flight evaluation of a miniature electrostatic accelerometer (MESA) for the measurement of low-level orbital accelerations was conducted. Measurements were obtained aboard an orbiting Saturn S-IVB stage in the AS-203 flight. All accelerometer flight data verified the principles of operation of the electrostatic accelerometer. Suspension was achieved with low cross-axis voltages with an apparent reduction in null bias from the value of $\pm 4 \times 10^{-4}$ g determined in laboratory testing with a 1-g environment. The sensitive-axis pulse constrainment operated properly and maintained the proof mass at the proper trigger level.

The difference between accelerometer data and the flight data based on thrust measurements cannot be explained; however, there is insufficient evidence to attribute the difference to errors in the accelerometer system. It is felt that a flight evaluation of a fully qualified flight model of the accelerometer is warranted by the results of this test. The apparent power failure experienced by the MESA early in the mission lifetime could possibly be attributed to the accelerometer's internal voltage regulating circuitry. Therefore, extensive environmental and electrical testing of the voltage regulator is deemed advisable before further flight use of the accelerometer.

A need for further flight experience with the accelerometer in an orbital environment is evident from these results. A reliable evaluation of the accuracy of the accelerometer requires in-flight calibration with input accelerations accurately described by other measurements.

Lewis Research Center,
National Aeronautics and Space Administration,
Cleveland, Ohio, August 15, 1967,
125-17-01-03-22.

REFERENCES

1. Meldrum, M. A.; Harrison, E. J.; and Milburn, Z.: Development of a Miniature Electrostatic Accelerometer (MESA) for Low g Applications. Rep. No. BAC-60009-509 (NASA CR-54137), Bell Aerosystems Co., Apr. 30, 1965.

2. Anon.: Evaluation of AS-203 Low Gravity Orbital Experiment. Tech. Rep. HSM-R421-67, Chrysler Corp., Jan. 13, 1967.

NASA-Langley, 1968 —— 14 E-4052

"The aeronautical and space activities of the United States shall be conducted so as to contribute . . . to the expansion of human knowledge of phenomena in the atmosphere and space. The Administration shall provide for the widest practicable and appropriate dissemination of information concerning its activities and the results thereof."

—NATIONAL AERONAUTICS AND SPACE ACT OF 1958

NASA SCIENTIFIC AND TECHNICAL PUBLICATIONS

TECHNICAL REPORTS: Scientific and technical information considered important, complete, and a lasting contribution to existing knowledge.

TECHNICAL NOTES: Information less broad in scope but nevertheless of importance as a contribution to existing knowledge.

TECHNICAL MEMORANDUMS: Information receiving limited distribution because of preliminary data, security classification, or other reasons.

CONTRACTOR REPORTS: Scientific and technical information generated under a NASA contract or grant and considered an important contribution to existing knowledge.

TECHNICAL TRANSLATIONS: Information published in a foreign language considered to merit NASA distribution in English.

SPECIAL PUBLICATIONS: Information derived from or of value to NASA activities. Publications include conference proceedings, monographs, data compilations, handbooks, sourcebooks, and special bibliographies.

TECHNOLOGY UTILIZATION PUBLICATIONS: Information on technology used by NASA that may be of particular interest in commercial and other non-aerospace applications. Publications include Tech Briefs, Technology Utilization Reports and Notes, and Technology Surveys.

Details on the availability of these publications may be obtained from:

SCIENTIFIC AND TECHNICAL INFORMATION DIVISION

NATIONAL AERONAUTICS AND SPACE ADMINISTRATION

Washington, D.C. 20546